Cell, Vol. 94, 727–737, September 18, 1998, Copyright ©1998 by Cell Press

Apaf1 (CED-4 Homolog) Regulates Programmed Cell Death in Mammalian Development

Francesco Cecconi,* Gonzalo Alvarez-Bolado,* Barbara I. Meyer,* Kevin A. Roth,† and Peter Gruss*‡
*Department of Molecular Cell Biology
Max Planck Institute of Biophysical Chemistry
D-37077 Göttingen
Germany
†Department of Pathology
Washington University School of Medicine
St. Louis, Missouri 63110

Summary

The cytosolic protein APAF1, human homolog of *C. elegans* CED-4, participates in the CASPASE 9 (CASP9)-dependent activation of CASP3 in the general apoptotic pathway. We have generated by gene trap a null allele of the murine *Apaf1*. Homozygous mutants die at embryonic day 16.5. Their phenotype includes severe craniofacial malformations, brain overgrowth, persistence of the interdigital webs, and dramatic alterations of the lens and retina. Homozygous embryonic fibroblasts exhibit reduced response to various apoptotic stimuli. In situ immunodetection shows that the absence of Apaf1 protein prevents the activation of Casp3 in vivo. In agreement with the reported function of CED-4 in *C. elegans*, this phenotype can be correlated with a defect of apoptosis. Our findings suggest that Apaf1 is essential for Casp3 activation in embryonic brain and is a key regulator of developmental programmed cell death in mammals.

Introduction

Apoptosis is an evolutionary conserved form of cell death regulated by several genes that play crucial roles in the development and homeostasis of multicellular organisms (Kerr et al., 1972; Jacobson et al., 1997).

In the nematode *C. elegans*, several genes have been isolated with negative and executive effects on the general apoptotic program, among them, *ced-9*, which inhibits cell death (Hengartner et al., 1992), and *ced-3* and *ced-4*, which promote cell death (Yuan and Horvitz, 1990, 1992).

Bcl2 represents the mammalian counterpart of CED-9 (Vaux et al., 1992; Hengartner and Horvitz, 1994) and is an integral membrane protein located mainly on the outer mitochondrial membrane (Krajewski et al., 1993). *Bcl2* belongs to a multigene family with several representatives in mammals (reviewed in Farrow and Brown, 1996; Reed, 1997; Newton and Strasser, 1998). *CED-3* encodes a protein 29% identical to human interleukin (IL)-1β-converting enzyme (ICE, Yuan et al., 1993), which belongs as well to a large family of related mammalian proteases termed caspases (*c*ysteine *asp*artate prote*ases*). These proteases initiate the apoptotic proteolytic cascade that leads, for instance, to activation of nucleases and cleavage of nuclear structural proteins (reviewed in Takahashi and Earnshaw, 1996).

Recently, a human CED-4 homolog has been isolated in HeLa cells and termed APAF1 (*a*poptotic *p*rotease *a*ctivating *f*actor 1; Zou et al., 1997). APAF1 participates in the cytochrome c/dATP-dependent activation of a mammalian CED-3 homolog, CASPASE 3 (CASP3) (also named CPP32, Xue et al., 1996; Zou et al., 1997), through the proteolytic activation of CASP9 (another CED-3 homolog; Duan et al., 1996; Li et al., 1997).

CED-4 has been determined to function downstream of CED-9 but upstream of CED-3 (Shaham and Horvitz, 1996). CED-3, CED-4, and CED-9 form a ternary complex in *C. elegans* (Chinnaiyan et al., 1997; Spector et al., 1997). Likewise, APAF1 functions downstream to Bcl2 (or its close family member $BclX_L$), which regulates the release of cytochrome c from mitochondria, but upstream of CASP3 (Zou et al., 1997). Besides, CASP9 and $BclX_L$ bind distinct regions of APAF1 forming also in mammalian cells a ternary complex (Pan et al., 1998).

The evolutionary conservation among *C. elegans* and vertebrates of the general apoptotic program at a biochemical and cellular level is thus evident, but the importance of apoptosis in animal development grows with organism complexity. Apoptosis-deficient nematodes can have a normal life span, although they have 15% more cells than normal animals and show a few functional deficiencies (Ellis et al., 1991; Jacobson et al., 1997). By contrast, mice in which Casp3 has been deleted by targeted disruption die perinatally with a massive cell overgrowth in the central nervous system, as a result of apoptosis deficiency in the neuroepithelial cells (Kuida et al., 1996). *BclX*-deficient mice die earlier, at embryonic day 13, exhibiting excess of apoptosis in brain, spinal cord, and hematopoietic system (Motoyama et al., 1995).

Apoptosis serves three functions in mammalian development (Glücksmann, 1951): deleting unneeded structures (phylogenetic apoptosis), controlling cell number (histogenetic apoptosis), and sculpting structures (morphogenetic apoptosis). It remains to be determined when and to which extent each protein member of the apoptotic program is involved in each of these processes. Obviously, Apaf1 is a good candidate to play a crucial role in mammalian development, for it interacts with $BclX_L$ and is upstream of Casp3.

To address these questions, we have taken advantage of the results of a gene trap study (Chowdhury et al., 1997) that has provided the means to isolate a null allele of the murine *Apaf1* gene. Here, we report the cloning of the mouse *Apaf1* cDNA and the analysis of embryonic phenotype in mice homozygous for this mutation. Our results indicate essential roles in vivo of Apaf1 in (1) regulating Casp3 activation, (2) establishing the proper development of brain structures, (3) controlling the cell number of retinal cell populations and lens polarization in eye development, (4) sculpting digits by eliminating

‡To whom correspondence should be addressed.

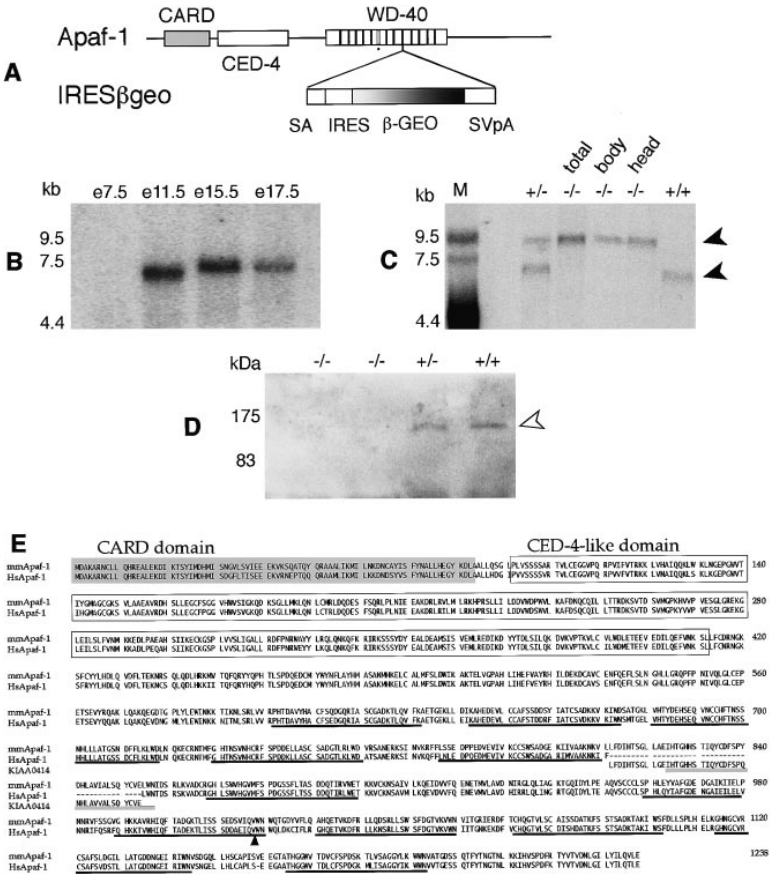

Figure 1. Generation of Apaf1-Deficient Embryos and Sequence of Apaf1 Protein

(A) Structure of the gene trap-vector/Apaf1 mRNA fused transcript. CARD, caspase recruitment domain; CED-4, CED-4-like domain; SA, splice acceptor site from *En2* gene; IRES, internal ribosomal entry site of the encephalomyocarditis virus; β-GEO, β-galactosidase fused to neomycin phosphotransferase; SVpA, SV40 polyadenylation site (Chowdhury et al., 1997).

(B) Northern blot of poly(A)+ RNA from mouse embryos at several developmental stages, hybridized with the 5′RACE product derived from the *Apaf1* gene trap line.

(C) Northern blot of poly(A)+ RNA from wild-type, homozygous, and heterozygous e14.5 embryos. Black arrowheads point to the endogenous (lower) and fusion (upper) transcripts.

(D) Western blot of protein extracts from wild-type, homozygous, and heterozygous e11.5 embryonic brains. Open arrowhead points to the endogenous Apaf1 protein band.

(E) Comparison of murine and human Apaf1 protein sequences. Gray box, CARD domain; white box, CED-4-like domain; underlined black, WD40 repeats; underlined gray (indicated by a dot in [A]), an additional WD40 repeat present in the mouse Apaf1 protein and deduced from the human KIAA0414 cDNA sequence (Ishikawa et al., unpublished data, GenBank accession number AB007873). Arrowhead, gene trap insertion site fusion transcript.

interdigital cells, and (5) leading the processes of secondary palate formation. These observations imply the possible involvement of Apaf1 in alternative cell death regulatory pathways.

Involvement of cell death genes in many human diseases has been shown in several cases (reviewed in Hoeppner et al., 1996). The localization of the *APAF1* gene on the long arm of human chromosome 12 suggests a role for this gene in Noonan syndrome (Jamieson et al., 1994).

Results and Discussion

Generation of a Null Allele of the Murine *Apaf1* Gene

In a large-scale gene trap screening program, we have isolated an embryonic stem (ES) cell clone trapping a gene that showed an interesting spatiotemporal expression pattern (see Figures 3–4). Using 5′RACE from the known reporter gene sequences, a 505-base-pair (bp) long fragment of the endogenous gene was cloned. The sequence of the 5′RACE product revealed a fusion of the reporter βgeo gene (β-galactosidase fused to neomycin phosphotransferase; Skarnes et al., 1992) to the murine homolog of *Apaf1* cDNA, 3′ downstream of the position encoding the amino acid (aa) 1018 (corresponding to number 975 of the 1194 aa composing the human protein; Zou et al., 1997). The insertion predicts the expression of a truncated Apaf1 protein and of the reporter protein βgeo (independently translated by means of an *i*nternal *r*ibosome *e*ntry *s*ite [IRES]), under the control of the *Apaf1* gene regulatory elements (Figure 1A).

Human APAF1 possesses an NH_2-terminal CED-3 prodomain–like region that includes a CARD (*ca*spase *r*ecruitment *d*omain), a CED-4-like segment, a COOH-terminal extension composed of multiple WD40 repeats that are lacking in the nematode CED-4 (Zou et al., 1997; Figure 1E). The insertion within the murine *Apaf1* occurred at the end of the region coding for the ninth of these repeats. As shown in experiments of in vitro reconstitution, the wild-type CASP9 translated in vitro binds to the CARD of APAF1 (Li et al., 1997). However, these data do not exclude the possibility that CASP9 interacts with other regions of APAF1 as well. Likewise, $BclX_L$ has been shown to bind a truncated APAF1 form that contained only the CED-4 homologous region (Pan et al., 1998). Therefore, CASP9 and $BclX_L$ bind to distinct domains in APAF1, consistent with the formation of a ternary complex. Finally, Zou et al. (1997) showed that APAF1 and CASP9 form a complex only in the presence of cytochrome c and dATP, which may induce conformational changes in APAF1 that expose its CARD.

The WD40 repeats at the COOH terminus are believed to mediate protein–protein interactions (Neer et al., 1994). Recently, the APAF1 WD40 domain has been shown to interact with $BclX_L$, but the meaning of this interaction is unknown (Hu et al., 1998). Moreover, deletion of the WD40 repeats renders APAF1 constitutively active and capable of processing CASP9 independent of cytochrome c and dATP (Srinivasula et al., 1998).

Table 1. Embryonic Lethality of *Apaf1* Insertional Mutation

Age (Days)	No. of Litters	Total Conceptuses	No. of Normal-Looking Embryos	Genotype of Embryos			No. of Abnormal Embryos
				+/+	+/−	−/−	
e10.5–11.0	1	12	12	5	5	2	0
e11.5–12.0	4	45	37	13	24	8	0
e12.5–13.0	2	19	14	4	10	5	5
e14.5–15.0	5	55	43	13	30	12	13
e16.5–17.0	4	43	39	11	28	4	4
e17.5–18.0	3	25	25	8	17	0	0
Total	19	199	170	54	114	31	22

Murine *Apaf1* mRNA is expressed at high levels from at least e11.5 to e17.5, as revealed by Northern blot analysis, and it is about 7.0 kb in size, in agreement with the reported dimension of its human counterpart (Figure 1B). Southern analysis of genomic DNA allowed the genotyping of an e14.5 litter (data not shown). Subsequent Northern blot analysis was used to identify relative levels of wild-type and fusion transcripts in wild-type, heterozygous, and homozygous embryos (Figure 1C). In the homozygotes, no endogenous *Apaf1* mRNA was detected, reflecting the absence of any splicing of the pre-mRNA transcribed from the mutant alleles around the newly inserted exons.

According to the insertional site, the mutant transcript (8.9 kb: 3.6 kb of the endogenous mRNA fused to 5.3 kb of the insertional vector mRNA) is predicted to code for two proteins; one of them would comprise (1) the CARD domain, (2) the CED-4-like domain, and (3) a truncated WD40 repeats domain of Apaf1; the second protein would consist of βgeo as the reporter product. To determine whether a truncated Apaf1 protein was present in the mutant homozygous embryos, we carried out immunoblotting experiments using antibodies raised to the NH_2 terminus of the human APAF1 protein. The anti-APAF1 antibody recognizes a protein that has an approximate molecular weight of 135 kDa. Analysis of protein extracts from an e12.5 litter is shown in Figure 1D. In the *Apaf1*$^{-/-}$ embryos, there was no detectable Apaf1 protein, as compared with the wild-type littermates. It is most likely that the truncated protein, if synthesized, is not stable and is rapidly degraded (Capecchi et al., 1974; Rechsteiner, 1987; Subramanian et al., 1995).

Cloning and Sequence of Murine *Apaf1* cDNA

We used the 5′RACE product to probe a murine e15.5 cDNA bank in order to clone the wild-type *Apaf1* message. The conceptual translation of the obtained 5227 bp long *Apaf1* cDNA sequence is shown in Figure 1E. Using the basic alignment tool (BLAST, Altschul et al., 1990), the entire length of the sequence was compared to the most commonly used databases. The 1238 aa protein is 88% homologous to the human APAF1 (Zou et al., 1997).

The gap of alignment between aa 811 and aa 855 among Apaf1 orthologs can be accounted for by the presence of a supplementary WD40 repeat in the mouse sequence; the human KIA00414 partial mRNA, identical to human *APAF1*, also contains this insertion (see Figure 1E).

Apaf1 Mutant Mice Develop Abnormally and Die before Birth

We examined about 200 embryos of the *Apaf1* gene trap line (Table 1). Abnormal embryos were found only at e12.5 and later. All abnormal embryos were homozygous for the *Apaf1* mutation, with only one exception; one wild-type e14.5 embryo showed exencephaly. The heterozygous animals were healthy and of normal size. No homozygous embryos were found beyond e16.5, suggesting that the *Apaf1* mutation is lethal around this age. The relative proportions of homozygous, heterozygous, and wild-type embryos found in our study are consistent with the expected Mendelian ratio. The phenotype of e12.5, e14.5, and e16.5 mutant embryos was analyzed and compared to the phenotype of the corresponding wild-type littermates.

Since no apparent discernible histological abnormalities were observed in the developing heart, lung, and liver (despite expression of *Apaf1* in these tissues in normal adult animals; data not shown), we focused on the craniofacial, eye, limb, and brain alterations.

Apaf1 Mutant Embryos Show Craniofacial Alterations

Fetuses (e16.5) homozygous for the *Apaf1* mutation show a characteristic craniofacial phenotype whose major traits are midline facial cleft, absence of skull vault, and of all vomer and ethmoidal elements, rostral exencephaly, and cleft palate (Figures 2A–2H). Targeted mutation of a number of genes has been reported to cause varying degrees of facial cleft, palatal cleft, or both (reviewed in Richman and Mitchell, 1996). None of these genes, however, encodes a component of the apoptotic machinery. Nevertheless, apoptosis has been hypothesized to play a key role in palatal fusion processes, where it would eliminate the medial edge epithelium of the secondary palatal shelves after they have contacted at e14.5 in the midline (reviewed in Ferguson, 1988). Accordingly, late and imperfect palatal fusion is a key component of the Apaf1 mutant phenotype (Figures 2C–2D). The basisphenoid bone, which is normally involved in the formation of the caudal third of the palate, shows an ossification defect in our mutants (Figures 2G–2H). It is tempting to speculate that proper fusion in the midline of the palate is an essential step for basisphenoid bone formation.

Our results suggest that apoptosis is essential in midline fusion of craniofacial structures. Since the Apaf1 mutant phenotype is the only apoptosis-deficient phenotype showing midline fusion defect, Apaf1 could be

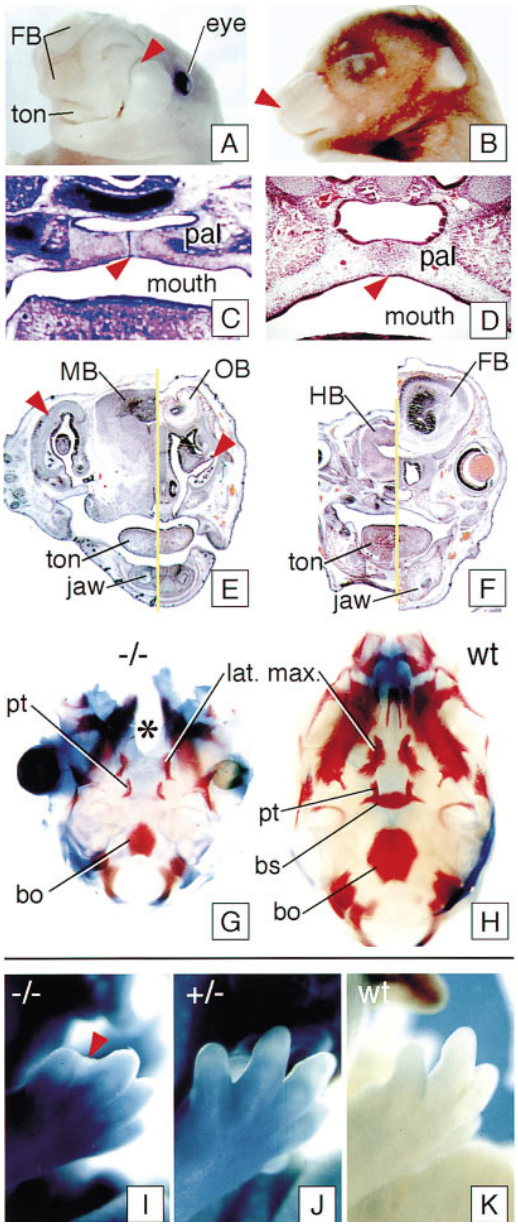

Figure 2. Craniofacial and Limb Phenotype of the *Apaf1*$^{-/-}$ Embryos

(A and B) Facial midline cleft and rostral exencephaly in a homozygous e16.5 fetus (A), as compared to a wild-type littermate (B). Red arrowheads, rostral border of the whisker pad. FB, forebrain; ton, tongue.

(C) Transversal section through the caudal third of the palate of an e14.5 homozygous embryo. The palatal shelves meet in the midline (arrowhead) but do not fuse. pal, secondary palate.

(D) Transversal section through the caudal third of the palate of an e14.5 wild-type embryo, showing complete fusion of the palatal shelves in the midline (arrowhead). pal, secondary palate.

(E) Composite figure comparing transverse sections through the rostral facial structures of a mutant e16.5 fetus (left) and a wild-type littermate (right). In the mutant, the brain separates the nasal cavities (arrowheads), while the tongue and jaw have a normal appearance. MB, midbrain; OB, olfactory bulb; ton, tongue.

(F) Composite figure comparing transverse sections through the caudal facial structures of a mutant e16.5 fetus (left) and a wild-type littermate (right). In the mutant, the skull is defective and the brain is grossly mispositioned. FB, forebrain; HB, hindbrain.

(G) Skeletal preparation of the skull of an e15.5 homozygous fetus; view from top. There is a large defect in the rostral two-thirds of the palate (asterisk), and the basisphenoid ossification point is absent.

(H) Wild-type littermate. The skull vault has been removed. bo, basioccipital; bs, basisphenoid; lat. max., lateral maxillary bone; pt, pterygoid bone.

(I, J, and K) Comparison of the right hands of e15.5 mouse fetuses reacted for detection of lacZ activity. The interdigital webs are persistent in the homozygous (arrowhead).

part of a specific apoptotic pathway involved in midline fusion.

Persistence of Interdigital Webs in Apaf1 Mutant Embryos

In wild-type and heterozygous embryos, the interdigital cells of the limbs, which undergo apoptosis as a means of sculpting the digits in many vertebrates (Saunders, 1966; reviewed in Jacobson et al., 1997), disappeared by e15.5; in the homozygotes at this stage, however, these cells can still be seen (Figures 2I–2K). Apoptosis was detected in situ by DNA fragmentation labeling (FragEL method) in the wild-type but only at a very low level in the homozygous interdigital cells (data not shown). These findings not only confirm in vivo the need for programmed cell death in the sculpting of the normal limb but also support the hypothesis that Apaf1 is a key component in apoptosis in multiple cell types.

Abnormal Eye Development in Apaf1 Mutant Embryos

Apaf1 mutants show alterations of the retina, lens, and eye vascular system. Already by e10.5 the retina shows Apaf1 expression (Figure 3A), although at that age the eye primordium of the mutant is morphologically normal. By e12.5, the retina of the mutant is noticeably thicker than the retina of the wild-type littermate (Figures 3B and 3C). At e14.5, the hyperplasic retina occupies most of the optic cup and is folded (Figures 3D and 3E). Programmed cell death has been described as a regulator of cell number (Bunt and Lund, 1981) during normal development of the retina (histogenetic cell death). Recently, it has been reported that two mechanisms of apoptosis coexist in the developing retina; one of these mechanisms is characteristic of retinal ganglion cells (Rehen et al., 1996). The specific expression of Apaf1 in the outermost layer of the developing retina (corresponding to the developing ganglion cell layer) suggests that this factor could be part of a ganglion cell–specific apoptotic pathway.

The lens of the Apaf1 mutant is smaller and seems incorrectly polarized. Programmed cell death has been reported to have a major role in lens morphogenesis (Silver and Hughes, 1973). The correct polarization of the lens depends probably on diffusible factors in the aqueous and vitreous (Coulombre and Coulombre, 1963). It is conceivable that alterations in the size and shape of the lens primordium subsequent to defective morphogenetic apoptosis lead to incorrect interaction with the environment and thus to incorrect polarization.

Apaf1 is expressed in the endothelial cells of the transient vascular system of the eye (hyaloid capillary system). By e14.5 vascular endothelial cells seem to obliterate completely the optic cup of the Apaf1 mutant (Figure

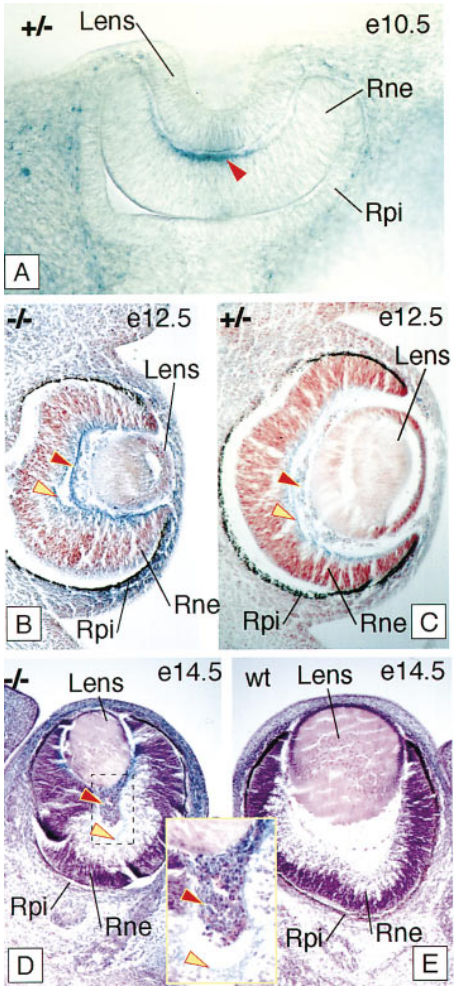

Figure 3. Eye Alterations in Apaf1 Mutants

(A) Vibratome section through the eye of an e10.5 heterozygous mouse embryo reacted for lacZ activity detection. Arrowhead, localized expression of Apaf1 in the neural retina. Rne, neural retina; Rpi, pigmented retina.

(B and C) The eye of the e12.5 homozygous embryo shows thickened retina and small lens (B) as compared to the eye of a heterozygous littermate (C). Embryos were reacted for lacZ activity detection before sectioning, and sections were counterstained with hematoxylin-eosin. Both homozygous and heterozygous show Apaf1 expression in the ganglion cell layer of the retina (yellow arrowheads) and in the endothelial cells of the vascular system (red arrowheads). Rne, neural retina; Rpi, pigmented retina.

(D and E) Sections through the eyes of homozygous (D) and heterozygous (E) e14.5 embryos. The homozygous retina is thicker, and the lens is smaller. Endothelial cells fill the optic cup in the homozygous. The portion framed in (D) is shown enlarged in the inset. Red arrowheads, endothelial cells; yellow arrowheads, ganglion cell layer. Rne, neural retina; Rpi, pigmented retina.

3D). This phenomenon suggests that apoptosis is necessary not only postnatally (reviewed in Lang, 1997) to eliminate the transient hyaloid capillary system but also to regulate the number of hyaloid capillaries already in the prenatal period. Alternatively, it is possible that the reduction in the size of the optic cup of the mutants (consequent to the abnormal increase in retinal thickness) is the cause of a concentration of the hyaloid capillaries in the center of the eye.

In summary, the Apaf1 phenotype underlines the three different functions of apoptosis in the eye, cell number regulation (histogenetic cell death, in the retina), morphogenetic cell death (lens), and elimination of a transient structure (phylogenetic cell death, in the hyaloid capillary system).

Brain Hyperplasia in Apaf1 Mutant Embryos

From e12.5 onward, the brain of the Apaf1 mutants shows important morphological distortion. The telencephalic vesicles seem abnormally folded and reduced in size, presumably due to the pressure exerted by the overgrown diencephalon and midbrain (Figures 4A and 4B). Anatomically, the brain hyperplasia found in our mutants is particularly intense in the diencephalon and midbrain; the convoluted mass of neuroepithelium and mantle that occupies the lumen of the midbrain (Figure 4C) is an abnormally enlarged choroid plexus of the fourth ventricle (hindbrain; Figure 4D). Histologically, the hyperplasia is localized to the mantle layer (differentiating compartment), especially in the diencephalon (Figure 4C). The ventricular layer (mitotic compartment) seems affected only in the choroid plexus. In this structure, not only the neuroepithelium is extensively overgrown and folded, but it is able to generate a mantle layer (Figure 4D), absent in wild-type animals. The medulla (hindbrain) is of normal appearance, and it is possible to identify nuclear primordia (Figure 4E). The cortical primordium is apparently delayed in development, but the size and organization of the ventricular layer seem normal (Figures 4F and 4G). The onset of this phenotype is an overgrowth of the ventral side of the hypothalamus insinuating itself through the cartilage of the base of the skull at e12.5. This phenomenon is most evident at e14.5 (Figure 4H). Consistently with this early defect, Apaf1 is expressed early in the ventral diencephalon (Figures 4I and 4J). Expression of Apaf1 as revealed by lacZ staining can also be seen in the early mantle of the basal ganglia (Figures 4I and 4K), in the neuroepithelium of the choroid plexus of the fourth ventricle (Figure 4L), and in the marginal layer of the hindbrain (Figures 4I and 4M) and spinal cord. The cause of the brain phenotype is presumably the lack of normal developmental programmed cell death in the mantle layer (differentiating compartment) of the diencephalon, midbrain, and cerebellum as well as in the ventricular layer (mitotic compartment) of the choroid plexus of the fourth ventricle. In wild-type animals, the choroid plexus is a region of neuroepithelium that does not generate a mantle layer but differentiates into an epithelial monolayer. Apoptosis is known to be a major normal developmental mechanism in the brain; in this organ, programmed cell death has mostly histogenetic functions (reviewed in Jacobson, 1991). The phenotypes caused by the targeted mutation of either of two other major genes related to programmed cell death agree with this view. Mouse embryos deficient in the *Casp3* gene show alterations in brain development due to lack of normal amount of programmed cell death (Kuida et al., 1996). Deficiency in $BclX_L$, an antiapoptotic protein, has as a result abnormally extensive death of neurons (Motoyama et al., 1995). In both cases the cell population affected by the mutation is the differentiating, postmitotic neurons of the mantle layer. The Apaf1

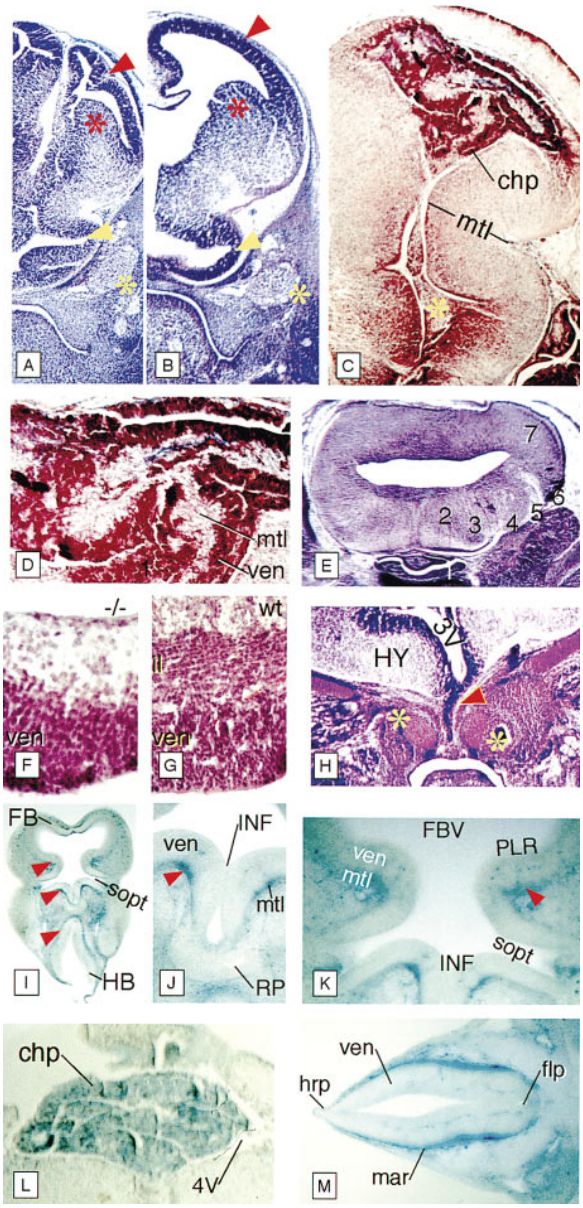

Figure 4. Brain Phenotype of Apaf1 Mutants

(A) Nissl-stained transverse section through the forebrain of an e12.5 homozygous mouse embryo showing folding of the cortex (red arrowhead) and deformation of the ganglionic eminence (red asterisk). The optic sulcus (yellow arrowhead) and trigeminal ganglion (yellow asterisk) are landmarks for comparison with (B). (B) Nissl-stained transverse section through the forebrain of a wild-type e12.5 embryo. Asterisks and arrowheads as in (A).

(C) Hematoxylin-eosin-stained transverse section through the diencephalon and rostral midbrain of an e14.5 homozygous embryo. The mantle layer (mtl) and choroid plexus (chp) show overgrowth and distorted shape. Ectopic masses of cells occupy the lumen (asterisk).

(D) Enlarged portion of (C) showing the overgrown choroid plexus. mtl, mantle layer; ven, ventricular layer.

(E) Nissl-stained section through the brain stem of an e16.5 homozygous fetus. 1, pituitary gland; 2, reticular nucleus; 3, facial nucleus; 4, principal nucleus of the trigeminal; 5, eighth cranial nerve; 6, cochlear nuclei; 7, cerebellum.

(F and G) Hematoxylin-eosin-stained sections through the cortex of e14.5 embryos, homozygous (F) and wild-type (G) for the Apaf1 mutation. The thickness and organization of the ventricular layer are comparable, although the homozygous seems delayed in development. ven, ventricular layer; il, intermediate layer; wt, wild type.

(H) Nissl-stained transverse section showing the ventral diencephalon of an e14.5 homozygous embryo. There is an abnormal growth of nervous tissue (arrowhead) insinuating itself through the base of the skull (asterisks).

(I) Transverse vibrotome section through the forebrain of an e10.5 heterozygous mouse embryo reacted for lacZ activity detection. The incipient mantle layers of the basal ganglia and ventral diencephalon, as well as the marginal layer of the hindbrain, are labeled (arrowheads). FB, forebrain; HB, hindbrain; sopt, optic sulcus.

(J) Detail of (I) showing Apaf1 expression in the mantle layer of the ventral diencephalon (arrowhead). INF, infundibulum; mtl, mantle layer; RP, Rathke's pouch; ven, ventricular layer.

(K) Detail of (I) showing Apaf1 expression in the mantle layer of the pallidal ridge (primordium of basal ganglia; arrowhead). FBV, forebrain ventricle; INF, infundibulum; mtl, mantle layer; PLR, pallidal ridge; sopt, optic sulcus; ven, ventricular layer.

(L) Transverse section through the fourth ventricle of an e14.5 homozygous embryo reacted for lacZ activity detection. The choroid plexus shows overgrowth and intense Apaf1 expression. 4V, fourth ventricle; chp, choroid plexus.

(M) Transverse section through the hindbrain of an e10.5 heterozygous mouse embryo reacted for lacZ activity detection. Apaf1 is expressed in the marginal layer. flp, floor plate; hrp, hindbrain roof plate; mar, marginal layer; ven, ventricular layer.

mutants, however, show both an excess of differentiating neurons in the mantle layer of midbrain and diencephalon and an abnormally large mitotic layer (ventricular layer) in the choroid plexus of the fourth ventricle. This suggests that Apaf1 has a role in morphogenetic as well as histogenetic programmed cell death in the developing nervous system.

The obliteration of the lumen of the neural tube could have as a consequence a degree of hydrocephalia. The enlarged brain, compounded by the defects of skull and the facial midline cleft and by the hydrocephalia, has as a final result the gross exencephaly found in Apaf1 mutants by e16.5 (Figures 2A and 2E).

Apaf1 Is Required for Activation of Casp3 In Vivo

The similarity of brain phenotypes in Apaf1 and Casp3 null mutations (Kuida et al., 1996; this work) strongly indicates that Apaf1 and Casp3 can be components of the same apoptotic pathway during brain development; this would be consistent with their functional interactions, already shown in vitro (Li et al., 1997; Zou et al., 1997). We have confirmed this hypothesis by means of immunostaining experiments carried out with the CM1 antibody on histological sections of wild-type and *Apaf1*$^{-/-}$ e12.5 embryos. The CM1 antibody, recently characterized (Srinivasan et al., 1998), recognizes only the cleaved 17 kDa subunit but not the 32 kDa proenzyme of Casp3. In the the wild-type central nervous system, we observed numerous CM1-immunoreactive cells (Figures 5A and 5B, 5E and 5F); positive neuritic processes were also readily identifiable (arrows in Figures 5E and 5F). In contrast, little if any CM1 immunoreactivity was detected in the e12.5 *Apaf1* homozygous brain (Figures 5C and 5D, 5G and 5H). Control studies performed on wild-type embryos showed no immunoreactivity in sections incubated without primary antibody. CM1 has previously been used to demonstrate Casp3

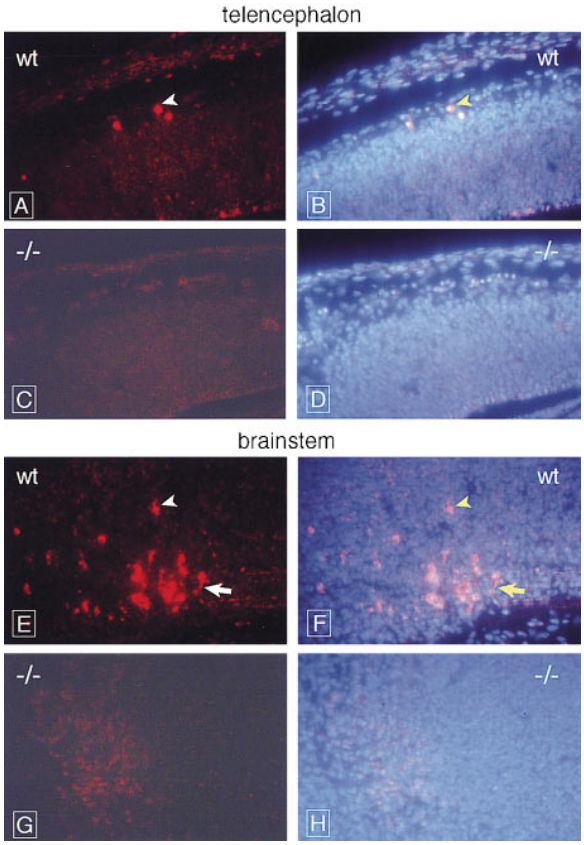

Figure 5. The Apaf1 Mutant Tissues Contain No Activated Casp3

Immunodetection of activated Casp3 by the CM1 antibody in the telencephalon (A–D) and brain stem (E–H) of wild-type (A, B, E, and F) and Apaf1 mutant (C, D, G, and H) e12.5 embryos. Activated Casp3–containing cells can be easily identified in the wild-type tissue, but not in the mutant. Four pairs of images are shown corresponding to four sections illuminated with differentially filtered UV light in order to demonstrate the specific fluorescent signal due to the antibody detection (A, C, E, and G) and the signal in the context of the tissue nonspecifically stained with bisbenzimide (B, D, F, and H). Arrowheads in (A), (B), (E), and (F) show examples of labeled cells in the wild-type tissue. Arrows in (E) and (F) show a labeled neuritic process. The brightness of (C) and (G) has been increased 25% with respect to the rest of the photographs in the panel.

activation in neurons undergoing programmed cell death; CM1 immunoreactivity is markedly increased in $BclX_L$-deficient embryos and decreased in Bax-deficient embryonic brain (Srinivasan et al., 1998). Recently, it has been reported that, as happens in *Apaf1* homozygous mutants and in Bax-deficient embryos, Casp9-deficient mice had little CM1 immunoreactivity in the developing nervous system and failed to activate Casp3 in a variety of experimental paradigms (Kuida et al., 1998). Together, these results indicate an in vivo apoptotic pathway whereby apoptotic stimuli trigger apoptosis, depending on the ratio of Bax:$BclX_L$ in neurons, through a multimolecular complex critically involving Apaf1 and Casp9 and ultimately leading to Casp3 activation and apoptosis. Disruption of any of the proapoptotic molecules in this pathway (Bax, Apaf1, Casp9, or Casp3) blocks the apoptotic cascade and leads to dramatically decreased programmed cell death (Deckwerth et al., 1996; Kuida et al., 1996, 1998; this work). These in vivo results confirm the in vitro reconstitution studies on the Apaf1 apoptotic cascade and further emphasize the parallel apoptotic pathways existing in *C. elegans* and mammals (Li et al., 1997; Zou et al., 1997).

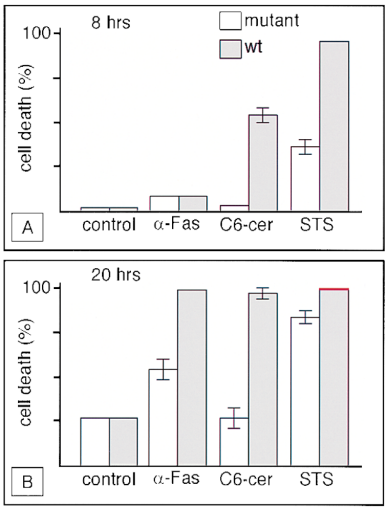

Figure 6. Susceptibility to Apoptosis of *Apaf1*$^{-/-}$ EFs

(A) Histogram showing the cell death percentage after 8 hr of treatment.

(B) Histogram showing the cell death percentage after 20 hr of treatment. The red line on top of the staurosporin/wild-type bar emphasizes the fact that the full effect of the inducer (100% cell death) was reached shortly after the first 8 hr (see [A]).

White, Apaf1 mutant cells; gray, wild-type cells. α-Fas, anti-Fas antibody; C6-cer, C6-ceramide; STS, staurosporin.

Interestingly, although Bax deficiency dramatically decreases neuronal programmed cell death, unlike Apaf1, Casp9, and Casp3-deficient embryos, brain overgrowth is not a feature of the *Bax*$^{-/-}$ nervous system (Knudson et al., 1995). Thus, Bax and $BclX_L$ may predominantly play a role in postmitotic neurons while the other molecules in this apoptotic pathway act on both neuronal progenitors and postmitotic cells.

Apaf1 Mutant Embryonic Fibroblasts Are Less Susceptible to Apoptotic Stimuli

To demonstrate the defect of apoptosis as the basis of this extensive phenotype, we examined the susceptibility of *Apaf1* homozygous embryonic fibroblasts (EFs), dissected from e13.5 embryos, to three different apoptotic stimuli in a time course experiment. *Apaf1* homozygous and wild-type EFs showed the expected divergent response to induction of apoptosis by anti-Fas antibody, C6-ceramide, and staurosporin, as revealed by morphological analysis (Figure 6).

The results can be summarized as follows: (1) After 8 hr of treatment with RMF2 anti-Fas antibody, no difference was observed between wild-type and homozygous EFs cell death rate (Figure 6A). Nevertheless, after a 20 hr long treatment, virtually all the wild-type EFs underwent apoptosis, while almost half of the Apaf1 mutant EFs were still alive (Figure 6B). (2) After an 8 hr long cell treatment with C6-ceramide, the second messenger in the sphingomyelin pathway, cell death was absent in

the Apaf1 mutant EFs, while apoptosis induction was effective in about 50% of the wild-type cells (Figure 6A). (3) Likewise, after 8 hr of treatment, staurosporin (STS), a broad-spectrum inhibitor of protein kinases that presumably acts downstream of receptors in signal transduction processes, induced cell death in about 95% of wild-type EFs but in only 30% of *Apaf1*$^{-/-}$ EFs (Figure 6A). Following prolonged treatment with both these reagents (C6-ceramide and STS), the differential response was proportionally confirmed (Figure 6B).

It has been shown that apoptotic defects due to Casp3 deficiency are remarkably stimulus-specific even within the same cell type, including EFs (Woo et al., 1998). Our results indicate that upstream pathways leading to Casp3 activation can be distinct and/or cross-communicating. For instance, the partial protective effect of Apaf1 deficiency to Fas-mediated apoptosis can be accounted for by the hypothesized cross-communication among two pathways of Casp3 activation, mitochondrial and Fas-mediated (Cryns and Yuan, 1998). Differential response can be caused as well by other Casp3-like proteases (Kuida et al., 1996; Woo et al., 1998). Similarly, the existence of other *Apaf1*-like genes cannot be excluded. These conclusions have been confirmed by Yoshida et al. (1998 [this issue of *Cell*]).

APAF1 Is a Candidate Gene Involved in Noonan Syndrome

To test the possibility that the *Apaf1* gene was located at sites of mouse spontaneous mutations and/or at sites associated with human syndromes, we mapped the *Apaf1* gene using fluorescent in situ hybridization (FISH) on normal mouse and human chromosome spreads. An *Apaf1* cDNA probe mapped on mouse chromosome 10, region C3-D1 and on human chromosome 12, q22-q23 (Figure 7). These results are in accordance with the predicted syntenic relationship between human and mouse chromosomes that share a region of homology in the distal part of their long arm (Copeland et al., 1990). This region is associated in mouse with forebrain overgrowth (fog), a spontaneous autosomal recessive mutation producing excessive growth or cellular proliferation in forebrain and midline cleft (Harris et al., 1997).

The human autosomal dominant Noonan syndrome (NS) has been associated with the region q22-qter of the long arm of human chromosome 12 (Jamieson et al., 1994). So far no obvious candidate gene for NS has been identified. This syndrome has a complicated clinical synopsis, mainly characterized by typical facial abnormalities, congenital cardiac defects, and limb malformations. In some cases the patients also show retinal degenerations as retinitis pigmentosa, which has been shown to be a degenerative disease related to apoptosis defect (Wong, 1994; Lorenzetti and Fryns, 1996). Therefore, *APAF1* can be considered as a candidate to be involved in NS.

Concluding Remarks

Apaf1, a key regulator of the apoptotic pathway, has a major role in developmental programmed cell death. Specifically, Apaf1 is involved in histogenetic cell death (control of cell number in the developing retina and brain), morphogenetic cell death (in the neural tube, lens, skull, face, and limbs), and phylogenetic cell death (elimination of the hyaloid artery system in the developing eye). Furthermore, Apaf1 is required for Casp3 activation in embryonic brain in vivo.

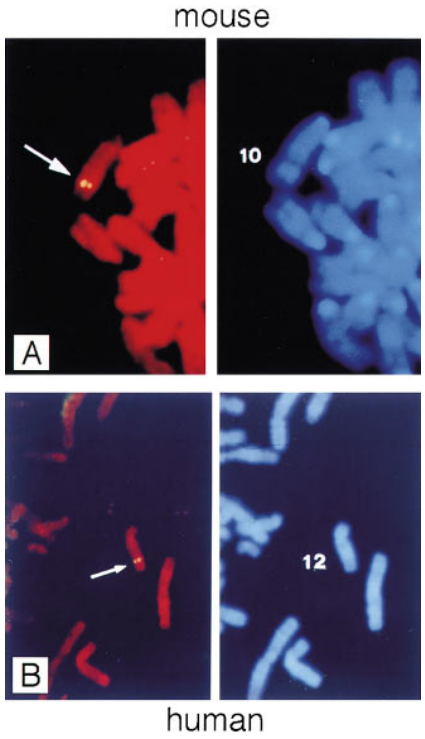

Figure 7. Chromosomal Localization of *Apaf1* in Mouse and Human

(A and B) Example of FISH mapping results for probe pϕ13.1 on mouse (A) and human (B) chromosomes. In both, the left panel shows the FISH signals on the chromosome, and the right panel shows the same mitotic figure stained with DAPI to identify mouse chromosome 10 (A) and human chromosome 12 (B). *Apaf1* probe maps on mouse chromosome 10, region C3-D1 and on human chromosome 12, q22-q23.

It has been described that APAF1, BclX_L, and CASP9 form in vitro a ternary complex, as well as their homologs CED-4, CED-9, and CED-3 in *C. elegans* (Pan et al., 1998), and that APAF1 is upstream of CASP3 (Zou et al., 1997). Targeted mutations in *BclX*, *Casp3*, and *Casp9* genes and the *Apaf1* mutation we generated induce major abnormalities in brain development, respectively due to excess and lack of cell death (Motoyama et al., 1995; Kuida et al., 1996, 1998; this work; Yoshida et al., 1998); these similarities together with the finding that Apaf1 is upstream to Casp3 in the apoptotic cascade imply the possibility of a functional connection between Apaf1, BclX_L, Casp9, and Casp3 during mouse development.

Nevertheless, in this study we have shown that Apaf1 is required in several other apoptotic processes in murine development and in multiple cell types. Our results imply that Apaf1 can be a key regulator of other apoptotic pathways, involving other caspases and/or Bcl2-like proteins, and raise the possibility that deficiencies in distinct developmental programmed cell death pathways can account for distinct phenotypes.

Finally, the phenotype of the Apaf1 mutant mice together with the chromosomal localization of *APAF1* gene in humans renders this gene a candidate to be mutated in Noonan syndrome.

Experimental Procedures

Generation of Apaf1-Deficient Mice and Cloning of Murine *Apaf1* cDNA

ES cell line GTXIX-18, containing an insertion of the gene trap vector IRESβgeo within the *Apaf1* gene, was generated as described (Chowdhury et al., 1997). The 5′RACE on ES cells RNA yielded 505 bp, upstream of the insertional splice acceptor site, that matched human *APAF1* sequence with 78% of nucleotide identities (Zou et al., 1997). This 505 bp long fragment was used as a probe to screen an e15.5 mouse cDNA library (Clontech), yielding several overlapping clones that were sequenced. A final consensus 5227 bp long, containing the entire 5′UTR and coding regions and partial 3′UTR regions of murine *Apaf1* cDNA, was obtained.

Founder chimeric males, generated as described from 129/Sv-derived ES cells (Chowdhury et al., 1997), were mated with outbred NMRI females, and heterozygous progenies were mated to maintain the allele.

Southern, Northern, and Western Analyses

A probe for *lacZ* sequences (LZ) was synthesized from an AvaI fragment of pCH110 (Pharmacia). A 213 bp long probe specific for the region immediately upstream to the insertional splice acceptor site (p13.02) spreading between position 2387 and 2600 of the mouse *Apaf1* cDNA was synthesized digesting plasmid pϕ13.1 (3.2 kb) with PstI. Probes LZ and p13.02 were used for genotyping by Southern blot analysis.

RNA blots containing 2 μg RNA per lane from different mouse adult tissues and embryonic stages were purchased from Clontech and probed with pϕ13.1. RNA poly(A)+ from *Apaf1*$^{-/-}$, *Apaf*$^{+/-}$, and *Apaf*$^{+/+}$ embryos was hybridized with pϕ13.1. Southern and Northern blots were hybridized with a 1.4 kb *Fkh-5* cDNA probe and a 2.0 kb β-*actin* cDNA probe, respectively, as internal controls.

Protein extracts were prepared from *Apaf1*$^{-/-}$, *Apaf1*$^{+/-}$, and *Apaf*$^{+/+}$ e10.5 brains, and Western blot analysis was performed using anti-APAF1 antibody (Santa Cruz Biotechnology) according to manufacturer's instructions.

Histological and Immunocytochemical Analyses

Whole-mount lacZ staining of embryos at different embryonic stages was performed as described (Gossler et al., 1989). For albumin-gelatin sectioning, the treated embryos were embedded in albumin-gelatin and vibratome sectioned into slices 40 μm thick. For paraffin sectioning specimens were impregnated with Paraffin wax (Paraplast Plus), embedded and transversally sectioned at 10 μm, and counterstained with neutral red, hematoxylin-eosin, or cresyl-violet.

A Klenow-FragEL DNA fragmentation detection kit (Calbiochem) was used to carry out the DNA fragmentation assay, following the conditions suggested by the manufacturer.

Skeletal preparations were carried out with alcian blue (cartilage) and alizarin red (bone) as described (Kessel and Gruss, 1991).

For CM1 immunostaining, paraffin-embedded horizontal brain sections from e12.5 wild-type and *Apaf1* homozygous mutants were deparaffinized and treated with blocking solution as described (Srinivasan et al., 1998). Rabbit anti-CM1 antibody (0.5 μg/ml) diluted in PBS-BB was applied overnight at 4°C and detected with biotin-conjugated donkey anti-rabbit serum (Jackson Immunoresearch Laboratories), horseradish peroxidase conjugated streptavidin (Jackson Immunoresearch Laboratories), and cyanine-3 tyramide deposition according to the manufacturer's protocol (NEN Life Sciences). Tissue was counterstained with bisbenzimide (Hoechst 33258; 0.2 μg/ml) and visualized on a Zeiss-Axioskop epifluorescence microscope.

Embryonic Fibroblasts Cell Death Induction

Embryonic fibroblasts were manually dissected from wild-type and homozygous e13.5 embryos, resuspended in Dulbecco's modified Eagle's medium (DMEM) supplemented with 5% fetal calf serum and gentamycin, and plated. Twenty-four hours after the initial plating, the cells were subjected to the following treatments at 37°C for 20 hr: anti-Fas antibody (RMF2 1 μg/ml, Immunotech), C6-ceramide (30 μM, BIOMOL), and Staurosporin (2 μM, BIOMOL). Pretreatment of the plated cells with 10 μg/ml cycloheximide was carried out in order to inhibit protein synthesis (Weil et al., 1996).

The cells were then analyzed by morphological criteria, and apoptotic events were counted after 8 hr and after 20 hr of treatment over ten photographic fields. The percentage of dying cells was calculated in comparison with a negative control plate.

Chromosomal Localization by FISH

The pϕ13.1 probe was labeled by nick translation using the BRL BioNick labeling kit (15°C, 1 hr), and the procedure for FISH detection was performed according to Heng et al. (1992) and Heng and Tsui (1993).

FISH signals and the DAPI banding pattern were recorded separately by taking photographs, and the assignment of the FISH mapping data with chromosomal bands was achieved by superimposing FISH signals with DAPI banded chromosomes (Heng and Tsui, 1993).

Under the conditions used, the hybridization efficiency was approximately 67% for this probe on the mouse chromosomes and 77% on the human chromosomes. After chromosome assignment, the detailed position was further determined based on the summary from ten photos.

Acknowledgments

We thank Dr. M. Kessel, Dr. A. Mansouri, Dr. A. Stoykova, Dr. G. Bernier, Dr. M. Salminen, Dr. M. Schwarz, J. Berger, A. De Antoni, and A. Pires for comments and suggestions. We are indebted to Dr. K. Chowdhury for the IRESβgeo vector. We thank Dr M. Piacentini (Rome) for helpful discussion. We acknowledge the excellent technical assistance of R. Altschäffel, A. Ficner, S. Hille, R. Libal, S. Mahsur, S. Schlott, T. Schulz, and A. Voigt. We also thank Dr. A. Srinivasan (IDUN Pharmaceuticals) for the generous gift of CM1 antiserum. Thanks are due to SeqLab (Göttingen) and seeDNA (Toronto) for DNA sequencing and chromosomal localization, respectively. This project was supported by Amgen, Inc. (Thousand Oaks, CA), by the Deutsche Forschungsgemeinschaft Leibniz-Program, and by the Max Planck Society. F. C. is supported by a Human Frontier Science Project Fellowship, and G. A.-B. is supported by a European Union Fellowship. K. A. R.'s lab is supported by National Institutes of Health grants NS35107 and NS35484.

Received May 21, 1998; revised August 3, 1998.

References

Altschul, S.F., Gish, W., Miller, W., Myers, E.W., and Lipman, D.J. (1990). Basic local alignment search tool. J. Mol. Biol. *215*, 403–410.

Bunt, S.M., and Lund, R.D. (1981). Development of a transient retinoretinal pathway in hooded and albino rats. Brain Res. *211*, 399–404.

Capecchi, M.R., Capecchi, N.E., Hughes, S.H., and Wahl, G.M. (1974). Selective degradation of abnormal proteins in mammalian tissue culture cells. Proc. Natl. Acad. Sci. USA *71*, 4732–4736.

Chinnaiyan, A.M., O'Rourke, K., Lane, B.R., and Dixit, V.M. (1997). Interaction of CED-4 with CED-3 and CED-9: a molecular framework for cell death. Science *275*, 1122–1126.

Chowdhury, K., Bonaldo, P., Torres, M., Stoykova, A., and Gruss, P. (1997). Evidence for the stochastic integration of gene trap vectors into the mouse germline. Nucleic Acids Res. *25*, 1531–1536.

Copeland, N.G., Gilbert, D.J., Cho, B.C., Donovan, P.J., Jenkins, N.A., Cosman, D., Anderson, D., Lyman, S.D., and Williams, D.E. (1990). Mast cell growth factor maps near the steel locus on mouse chromosome 10 and is deleted in a number of steel alleles. Cell *63*, 175–183.

Coulombre, J.L., and Coulombre, A.J. (1963). Lens development: fiber elongation and lens orientation. Science *142*, 1489–1490.

Cryns, V., and Yuan, J. (1998). Proteases to die for. Genes Dev. *12*, 1551–1570.

Deckwerth, T.L., Elliott., J.L., Knudson, C.M., Johnson, Jr., E.M., Snider, W.D., and Korsmeyer, S.J. (1996). BAX is required for neuronal death after trophic factor deprivation and during development. Neuron *17*, 401–411.

Duan, H., Orth, K., Chinnaiyan, A.M., Poirier, G.G., Froelich, C.J., He, W.W., and Dixit, V.M. (1996). ICE-LAP6, a novel member of the ICE/Ced-3 gene family, is activated by the cytotoxic T cell protease granzyme B. J. Biol. Chem. *271*, 16720–16724.

Ellis, R.E., Yuan, J.Y., and Horvitz, H.R. (1991). Mechanisms and functions of cell death. Annu. Rev. Cell Biol. *7*, 663–698.

Farrow, S.N., and Brown, R. (1996). New members of the Bcl-2 family and their protein partners. Curr. Opin. Genet. Dev. *6*, 45–49.

Ferguson, M.W. (1988). Palate development. Development *103* Suppl., 41–60.

Glücksmann, A. (1951). Cell deaths in normal vertebrate ontogeny. Biol. Rev. *26*, 59–86.

Gossler, A., Joyner, A.L., Rossant, J., and Skarnes, W.C. (1989). Mouse embryonic stem cells and reporter constructs to detect developmentally regulated genes. Science *244*, 463–465.

Harris, B.S., Franz, T., Ullrich, S., Cook, S., Bronson, R.T., and Davisson, M.T. (1997). Forebrain overgrowth (fog): a new mutation in the mouse affecting neural tube development. Teratology *55*, 231–240.

Heng, H.H., and Tsui, L.C. (1993). Modes of DAPI banding and simultaneous in situ hybridization. Chromosoma *102*, 325–332.

Heng, H.H., Squire, J., and Tsui, L.C. (1992). High-resolution mapping of mammalian genes by in situ hybridization to free chromatin. Proc. Natl. Acad. Sci. USA *89*, 9509–9513.

Hengartner, M.O., and Horvitz, H.R. (1994). *C. elegans* cell survival gene *ced-9* encodes a functional homolog of the mammalian proto-oncogene *bcl-2*. Cell *76*, 665–676.

Hengartner, M.O., Ellis, R.E., and Horvitz, H.R. (1992). *Caenorhabditis elegans* gene *ced-9* protects cells from programmed cell death. Nature *356*, 494–499.

Hoeppner, D.J., Hengartner, M.O., and Fisher, D.E. (1996). Programmed cell death: from development to disease. Biochim. Biophys. Acta *1242*, 217–220.

Hu, Y., Benedict, M.A., Wu, D., Inohara, N., and Nunez, G. (1998). Bcl-XL interacts with Apaf-1 and inhibits Apaf-1-dependent caspase-9 activation. Proc. Natl. Acad. Sci. USA *95*, 4386–4391.

Jacobson, M. (1991). Developmental Neurobiology, 3rd edition. (New York: Plenum Press).

Jacobson, M.D., Weil, M., and Raff, M.C. (1997). Programmed cell death in animal development. Cell *88*, 347–354.

Jamieson, C.R., van der Burgt, I., Brady, A.F., van Reen, M., Elsawi, M.M., Hol, F., Jeffery, S., Patton, M.A., and Mariman, E. (1994). Mapping a gene for Noonan syndrome to the long arm of chromosome 12. Nature Genet. *8*, 357–360.

Kerr, J.F., Wyllie, A.H., and Currie, A.R. (1972). Apoptosis: a basic biological phenomenon with wide-ranging implications in tissue kinetics. Br. J. Cancer *26*, 239–257.

Kessel, M., and Gruss, P. (1991). Homeotic transformations of murine vertebrae and concomitant alteration of Hox codes induced by retinoic acid. Cell *67*, 89–104.

Knudson, C.M., Tung, K.S.K., Tourtellotte, W.G., Brown, G.A.J., and Korsmeyer, S.J. (1995). Bax-deficient mice with lymphoid hyperplasia and male germ cell death. Science *270*, 96–99.

Krajewski, S., Tanaka, S., Takayama, S., Schibler, M.J., Fenton, W., Reed, J.C. (1993). Investigation of the subcellular distribution of the bcl-2 oncoprotein: residence in the nuclear envelope, endoplasmic reticulum, and outer mitochondrial membranes. Cancer Res. *53*, 4701–4714.

Kuida, K., Zheng, T.S., Na, S., Kuan, C., Yang, D., Karasuyama, H., Rakic, P., and Flavell, R.A. (1996). Decreased apoptosis in the brain and premature lethality in CPP32-deficient mice. Nature *384*, 368–372.

Kuida, K., Haydar, T.F., Kuan, C.-Y., Gu, Y., Taya, C., Karasuyama, H., Su, M.S.-S., Rakic, P., and Flavell, R.A. (1998). Reduced apoptosis and cytochrome c-mediated caspase activation in mice lacking Caspase 9. Cell *94*, 325–337.

Lang, R.A. (1997). Apoptosis in mammalian eye development: lens morphopgenesis, vascular regression and immune privilege. Cell Death Diff. *4*, 12–20.

Li, P., Nijhawan, D., Budihardjo, I., Srinivasula, S.M., Ahmad, M., Alnemri, E.S., and Wang, X. (1997). Cytochrome c and dATP-dependent formation of Apaf-1/caspase-9 complex initiates an apoptotic protease cascade. Cell *91*, 479–489.

Lorenzetti, M.E., and Fryns, J.P. (1996). Retinitis pigmentosa in a young man with Noonan syndrome: further evidence that Noonan syndrome (NS) and the cardio-facio-cutaneous syndrome (CFC) are variable manifestations of the same entity? Am. J. Med. Genet. *65*, 97–99.

Motoyama, N., Wang, F., Roth, K.A., Sawa, H., Nakayama, K., Nakayama, K., Negishi, I., Senju, S., Zhang, Q., Fujii, S., and Loh, D.Y. (1995). Massive cell death of immature hematopoietic cells and neurons in Bcl-x-deficient mice. Science *267*, 1506–1510.

Neer, E.J., Schmidt, C.J., Nambudripad, R., and Smith, T.F. (1994). The ancient regulatory-protein family of WD-repeat proteins. Nature *371*, 297–300.

Newton, K., and Strasser, A. (1998). The Bcl-2 family and cell death regulation. Curr. Opin. Genet. Dev. *8*, 68–75.

Pan, G., O'Rourke, K., and Dixit, V.M. (1998). Caspase-9, Bcl-XL, and Apaf-1 form a ternary complex. J. Biol. Chem. *273*, 5841–5845.

Rechsteiner, M. (1987). Ubiquitin mediated pathways for intracellular proteolysis. Annu. Rev. Cell Biol. *3*, 1–30.

Reed, J.C. (1997). Double identity for proteins of the Bcl-2 family. Nature *387*, 773–776.

Rehen, S.K., Varella, M.H., Freitas, F.G., Moraes, M.O., and Linden, R. (1996). Contrasting effects of protein synthesis inhibition and of cyclic AMP on apoptosis in the developing retina. Development *122*, 1439–1448.

Richman, J., and Mitchell, P.J. (1996). Craniofacial development: knockout mice take one on the chin. Curr. Biol. *6*, 364–367.

Saunders, J.W., Jr. (1966). Death in embryonic systems. Science *154*, 604–612.

Shaham, S., and Horvitz, H.R. (1996). An alternatively spliced *C. elegans* ced-4 RNA encodes a novel cell death inhibitor. Cell *86*, 201–208.

Silver, J., and Hughes, F.W. (1973). The role of cell death during morphogenesis of the mammalian eye. J. Morph. *140*, 159–170.

Skarnes, W.C., Auerbach, B.A., and Joyner, A.L. (1992). A gene trap approach in mouse embryonic stem cells: the lacZ reported is activated by splicing, reflects endogenous gene expression, and is mutagenic in mice. Genes Dev. *6*, 903–918.

Spector, M.S., Desnoyers, S., Hoeppner, D.J., and Hengartner, M.O. (1997). Interaction between the *C. elegans* cell-death regulators CED-9 and CED-4. Nature *385*, 653–656.

Srinivasan, A., Roth, K.A., Sayers, R.O., Shindler, K.S., Wong, A.M., Fritz, L.C., and Tomaselli, K.J. (1998). *In situ* immunodetection of activated caspase-3 in apoptotic neurons in the developing nervous system. Cell Death Diff., in press.

Srinivasula, S.M., Ahmad, M., Fernandes-Alnemri, T., and Alnemri, E.S. (1998). Autoactivation of procaspase-9 by Apaf-1-mediated oligomerization. Mol. Cell *1*, 949–957.

Subramanian, V., Meyer, B.I., and Gruss, P. (1995). Disruption of the murine homeobox gene *Cdx1* affects axial skeletal identities by altering the mesodermal expression domains of *Hox* genes. Cell *83*, 641–653.

Takahashi, A., and Earnshaw, W.C. (1996). ICE-related proteases in apoptosis. Curr. Opin. Genet. Dev. *6*, 50–55.

Vaux, D.L., Weissman, I.L., and Kim, S.K. (1992). Prevention of programmed cell death in *Caenorhabditis elegans* by human bcl-2. Science *258*, 1955–1957.

Weil, M., Jacobson, M.D., Coles, H.S., Davies, T.J., Gardner, R.L., Raff, K.D., and Raff, M.C. (1996). Constitutive expression of the machinery for programmed cell death. J. Cell Biol. *133*, 1053–1059.

Wong, P. (1994). Apoptosis, retinitis pigmentosa, and degeneration. Biochem. Cell. Biol. *72*, 489–498.

Woo, M., Hakem, R., Soengas, M.S., Duncan, G.S., Shahinian, A., Kagi, D., Hakem, A., McCurrach, M., Khoo, W., Kaufman, S.A., et al. (1998). Essential contribution of caspase 3/CPP32 to apoptosis and its associated nuclear changes. Genes Dev. *12*, 806–819.

Xue, D., Shaham, S., and Horvitz, H.R. (1996). The *Caenorhabditis elegans* cell-death protein CED-3 is a cysteine protease with substrate specificities similar to those of the human CPP32 protease. Genes Dev. *10*, 1073–1083.

Yoshida, H., Kong, Y.-Y., Yoshida, R., Elia, A.J., Hakem, A., Hakem, R., Penninger, J.M., and Mak, T.W. (1998). Apaf1 is required for mitochondrial pathways of apoptosis and brain development. Cell *94*, this issue, 739–750.

Yuan, J.Y., and Horvitz, H.R. (1990). The *Caenorhabditis elegans* genes *ced-3* and *ced-4* act cell autonomously to cause programmed cell death. Dev. Biol. *138*, 33–41.

Yuan, J., and Horvitz, H.R. (1992). The *Caenorhabditis elegans* cell death gene ced-4 encodes a novel protein and is expressed during the period of extensive programmed cell death. Development *116*, 309–320.

Yuan, J., Shaham, S., Ledoux, S., Ellis, H.M., and Horvitz, H.R. (1993). The *C. elegans* cell death gene *ced-3* encodes a protein similar to mammalian interleukin-1 beta-converting enzyme. Cell *75*, 641–652.

Zou, H., Henzel, W.J., Liu, X., Lutschg , A., and Wang, X. (1997). Apaf-1, a human protein homologous to *C. elegans* CED-4, participates in cytochrome c-dependent activation of caspase-3. Cell *90*, 405–413.

GenBank Accession Number

The accession number for the nucleotide sequence of murine *Apaf1* is AF064071.